

# Comparison of 2D and 3D wavelet features for TLE lateralization

Kouros Jafari-Khouzani,<sup>\*a,b</sup> Hamid Soltanian-Zadeh,<sup>b,c</sup> Kost Elisevich<sup>d</sup>, Suresh Patel<sup>e</sup>

<sup>a</sup>Computer Science Department, Wayne State University, Detroit, MI 48202, USA

<sup>b</sup>Radiology Image Analysis Lab., Henry Ford Health System, Detroit, MI 48202, USA

<sup>c</sup>Electrical and Computer Engineering Dept., University of Tehran, Tehran 14395, Iran

<sup>d</sup>Neurosurgery Dept., Henry Ford Health System, Detroit, MI 48202, USA

<sup>e</sup>Radiology Dept., Henry Ford Health System, Detroit, MI 48202, USA

## ABSTRACT

Intensity and volume features of the hippocampus from MR images of the brain are known to be useful in detecting the abnormality and consequently candidacy of the hippocampus for temporal lobe epilepsy surgery. However, currently, intracranial EEG exams are required to determine the abnormal hippocampus. These exams are lengthy, painful and costly. The aim of this study is to evaluate texture characteristics of the hippocampi from MR images to help physicians determine the candidate hippocampus for surgery. We studied the MR images of 20 epileptic patients. Intracranial EEG results as well as surgery outcome were used as gold standard. The hippocampi were manually segmented by an expert from T1-weighted MR images. Then the segmented regions were mapped on the corresponding FLAIR images for texture analysis. We calculate the average energy features from 2D wavelet transform of each slice of hippocampus as well as the energy features produced by 3D wavelet transform of the whole hippocampus volume. The 2D wavelet transform is calculated both from the original slices as well as from the slices perpendicular to the principal axis of the hippocampus. In order to calculate the 3D wavelet transform we first rotate each hippocampus to fit it in a rectangular prism and then fill the empty area by extrapolating the intensity values. We combine the resulting features with volume feature and compare their ability to distinguish between normal and abnormal hippocampi using linear classifier and fuzzy c-means clustering algorithm. Experimental results show that the proposed texture features can correctly classify the hippocampi.

**Keywords:** Epilepsy, medical image processing, texture analysis, wavelet transform

## 1. INTRODUCTION

Localization of the abnormal zones in the brain is an important task in the treatment of temporal lobe epilepsy. More than 20% of the epileptic patients undergo surgery when treatment with medication is ineffective. The conventional gold standard method (phase I) of evaluating an epileptic patient for surgical candidacy requires EEG exams to detect irritative zones, which is lengthy, painful, and costly. If the epileptic foci is not sufficiently localized in phase I, the patient will need to undergo phase II of the surgical evaluation, which involves implantation of electrodes intracranially and monitoring the patient for nearly two weeks.

It has been shown that the determination of structural and volumetric asymmetries in the human brain from MR images provides critical data for the diagnosis of focal abnormality. The hippocampus is an important component of the human brain's limbic system. The variations in volume and architecture of the hippocampus have been observed with some brain diseases such as schizophrenia, epilepsy, and Alzheimer.<sup>1,2</sup> There have been some attempts to employ texture analysis of MR images for characterization of different diseases. In some applications, texture properties are used to discriminate the normal and abnormal tissues. In fact, there is a probability that we may be able to discriminate different tissues based on texture properties. For example, studies of intracranial tumors have demonstrated that MR image texture may be used to determine the tumor type.<sup>3</sup> In this section we review some of the applications of texture analysis techniques to discriminate different tissues in MR images.

---

\* Correspondences to: [kjafari@rad.hfh.edu](mailto:kjafari@rad.hfh.edu), [hamids@rad.hfh.edu](mailto:hamids@rad.hfh.edu). URL: <http://radiologyresearch.org>

In our early work<sup>4</sup> we used multiwavelet texture features to specify the candidate hippocampus for surgery in temporal lobe epilepsy (TLE). Herlidou et al. use texture analysis methods for the diagnosis of skeletal muscle dystrophy in MR images<sup>5</sup> and evaluation of bone structure of the calcaneus of osteoporotic patients.<sup>6</sup> The texture analysis was performed using four statistical methods: histogram, co-occurrence matrix, gradient matrix, and runlength matrix (references<sup>5,6</sup>) and one structural method: mathematical morphology (reference<sup>5</sup>) along with correspondence factorial analysis (CFA). Reuze et al.<sup>7</sup> use four classes of textural features: fractal, co-occurrence, high order statistics and mathematical morphology, to detect muscle disease (myopathy) from MR images. They concluded that mathematical morphology results in the best classification rate.

Freeborough and Fox<sup>8</sup> use texture analysis for diagnosis and tracking of Alzheimer's disease (AD) from MR images of the brain. Texture is quantified over all coronal slices of the brain region using co-occurrence matrices for angles of 0°, 45°, 90°, and 135° and for 10 different displacement vectors. Duchesne et al.<sup>9</sup> employ texture analysis to classify the temporal lobe epilepsy using MR image appearance. They use a volume of interest (VOI) around the hippocampus instead of hippocampus alone. For classification of the images, models of the intensity characteristics and shape deformations of the VOI are constructed and concatenated into an appearance model for the volume. For the VOI with  $n$  pixels, they consider an  $n$ -dimensional space and use the principal component analysis (PCA) to find the eigenvectors as orthonormal bases spanning  $n$ -dimensional allowable space. In this way they consider both gray-level intensities and shape deformations.

Yu et al.<sup>10</sup> try to detect epilepsy by texture analysis of MR brain images in the lithium-pilocarpine rat model. They use three texture parameters derived from co-occurrence matrix to characterize structural abnormalities. Bernasconi et al.<sup>11</sup> study the first-order and second-order texture features to assess structural integrity of mesial temporal lobe structures (hippocampus, amygdala, and entorhinal cortex). They do a similar texture analysis work for temporopolar cortex and white matter in TLE by incorporating volumetric measurements.<sup>12</sup> Yu et al.<sup>13</sup> use first-order and second-order texture features to detect abnormality of the hippocampus in temporal lobe epilepsy. Segovia-Martinez et al.<sup>14</sup> use the method of gray-level dependence histograms (GLDH) and derive texture anisotropy features from MRI data that correlate with the result of Mini Mental State Examination (MMSE), which routinely helps to diagnosis Alzheimer's disease. Mahmoud-Ghoneim et al.<sup>15</sup> propose a 3D texture analysis approach using the co-occurrence matrix for brain tumor characterization. Herlidou et al.<sup>16</sup> employ first order, second order, and runlength matrix for different ROIs of the brain for characterization of healthy and pathologic human brain tissues. Bonilha et al.<sup>17</sup> use co-occurrence and runlength matrices to detect hippocampal abnormalities in patients with pathologically proven hippocampal sclerosis.

In this paper, in addition to volumetry, we analyze the MRI signal (image gray levels) in each hippocampus to get a sensitive and specific means for determining the site of partial epilepsy of mesial temporal origin. We use the 3D T1-weighted images of the brain to manually segment the hippocampus structure, and the corresponding 3D FLAIR images to get textural information of each hippocampus. We calculate the average energy features from 2D wavelet transform of each slice of hippocampus as well as the energy features produced by 3D wavelet transform of the whole hippocampus volume. After calculating the vector of features for a set of patients, we examine the ability of linear classifier and fuzzy c-means clustering algorithm to classify them into two groups of right and left abnormal hippocampi. The methods developed in this project are evaluated by the current gold standard of EEG phase II studies.

## 2. METHODS

### 2.1. Wavelet Transform

Wavelet transform provides a spatial/frequency representation of a signal. Wavelet coefficients of a signal  $f(t)$  are the projections of the signal onto the multiresolution subspaces  $V_j = \overline{\text{span}\{\varphi_{j,k}(t), k \in \mathbb{Z}\}}$  and  $W_j = \overline{\text{span}\{\psi_{j,k}(t), k \in \mathbb{Z}\}}$ ,  $j \in \mathbb{Z}$  where the basis functions  $\varphi_{j,k}(t)$  and  $\psi_{j,k}(t)$  are constructed by dyadic dilations and translations of the scaling and wavelet functions  $\varphi(t)$  and  $\psi(t)$ :

$$\varphi_{j,k}(t) = 2^{j/2} \varphi(2^j t - k) \quad (1)$$

$$\psi_{j,k}(t) = 2^{j/2} \psi(2^j t - k) \quad (2)$$

The scaling and wavelet functions satisfy the dilation and wavelet equations:

$$\varphi(t) = \sqrt{2} \sum_n h(n) \varphi(2t - n) \tag{3}$$

$$\psi(t) = \sqrt{2} \sum_n g(n) \varphi(2t - n) \tag{4}$$

where  $n \in Z$ . For any function  $f(t) \in L^2(\mathfrak{R})$  we have:

$$f(t) = \sum_k c_{J_0,k} \varphi_{J_0,k}(t) + \sum_{j=J_0}^{\infty} \sum_k d_{j,k} \psi_{j,k}(t) \tag{5}$$

Having the coefficients  $c_{j,k}$  and  $d_{j,k}$  at a specific level  $j$  we can calculate the coefficients at level  $j-1$  using a filter bank as shown in Fig. 1. In this figure, two levels of decomposition are depicted. H and G are lowpass and highpass filters corresponding to the coefficients  $h(n)$  and  $g(n)$  respectively. The wavelet decomposition of a 2D signal can be achieved by applying the 1D wavelet decomposition along the rows and columns of the image separately.<sup>18</sup> Fig. 2 shows the frequency subbands resulted from two levels of decomposition of an image. Wavelet transform of a 3D signal can be achieved by applying the 1D wavelet transform along all the three directions. The resulted frequency subbands for two levels of decomposition are shown in Fig. 3.

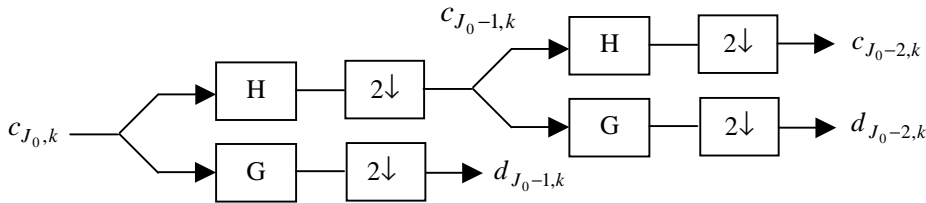


Fig. 1. The filter bank for calculating the wavelet coefficients.

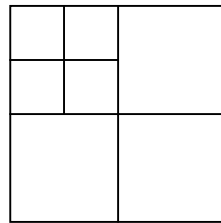


Fig. 2. Frequency subbands produced by two levels of wavelet decomposition of an image.

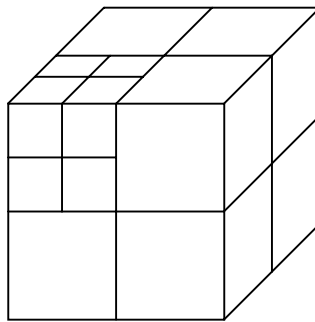


Fig. 3. Frequency subbands produced by two levels of wavelet decomposition of a 3D image.

## 2.2. Wavelet Features

For each submatrix in Fig.2, we calculate the following features:

$$\text{energy} = \frac{1}{M \times N} \sum_{x=1}^M \sum_{y=1}^N I^2(x, y) \quad (6)$$

$$\text{entropy} = \frac{-1}{M \times N} \sum_{x=1}^M \sum_{y=1}^N \left( \frac{I^2(x, y)}{\text{norm}^2} \right) \log \left( \frac{I^2(x, y)}{\text{norm}^2} \right) \quad (7)$$

where  $I(x, y)$  shows the submatrix elements and  $M$  and  $N$  are the dimensions of each submatrix and  $\text{norm}^2 = \sum_x \sum_y I^2(x, y)$ . Similarly we can define the energy and entropy features for the 3D subbands in Fig. 3.

## 2.3. Classification

We employ two kinds of classifiers: linear classifier, which is supervised and can be easily implemented by a neural network, and fuzzy c-means classifier, which is unsupervised. Fig. 4 shows the corresponding neural network for linear classifier. As shown in this figure, this neural network has a two-value output, which shows either left or right hippocampus is abnormal. The weighted sum of the features plus a bias is the discriminant function. To determine how effectively the classes are separated, we use the EEG phase II results as the gold standard and compute the correct classification percentages by counting the misclassified hippocampi.

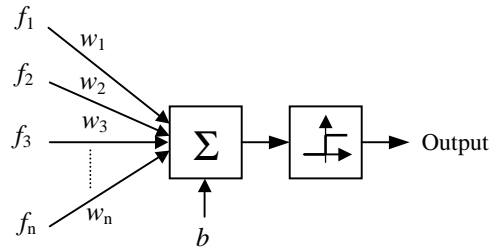


Fig. 4. The linear classifier.

## 3. PRACTICAL CONSIDERATIONS

In practice we face some problems for texture analysis of MR images. Some of these problems are as follows:

1. The regions of interest (ROIs) in patients are not all from the same size, while in texture classification experiments authors usually use images of the same size (the extracted features may be dependent on the image size). This may make some texture classification methods inappropriate for MR images.
2. The ROI does not always have a rectangular shape. In some texture classification techniques (like wavelet transform) we need a rectangular shape of the image. If we choose a rectangular area inside the ROI, we may lose some information outside this rectangle. If we inscribe the ROI in a rectangle, we need to assign some intensity values to the pixels outside the ROI but inside the rectangle. If we set all these points to zero, the produced sharp edges may significantly affect the extracted feature values. In this paper we fill the empty area using the proposed method in reference<sup>4</sup>. The hippocampus volume is inscribed in a rectangular prism and the empty area is filled by repeated dilation and averaging for all its 2D slices as depicted in Figs. 5 and 6. The hippocampus is characterized from the coronal slices of the brain. In order to inscribe the hippocampus volume in a rectangular prism, we can use the method of principal component analysis to find the principal axis of the hippocampus. Then by shifting and rotation we can inscribe the hippocampus in a rectangular prism, and find the pixel values of the new points by interpolation. In this way the empty area of the 3D image to be filled, will become minimum.

3. To deal with a 3D ROI, we need to develop algorithms for 3D texture analysis. We may make a number of slices of the 3D image and evaluate each slice separately. In this paper, we compare the 2D and 3D wavelet characterization of the hippocampi images.
4. Textures in medical images do not appear as periodic and uniform patterns as in synthetic textures. Therefore not all the successful texture analysis techniques are suitable for MR images.
5. In practice we need to first segment the image into the desired regions of interest. The result of texture characterization will be affected by the segmentation result. If the segmentation is not accurate and repeatable, the texture analysis result will not be reliable. In this paper, the images were segmented carefully by an expert. The sagittal and coronal views of a sample of manual segmentation are shown in Fig. 7.

Like our previous work in reference<sup>4</sup>, an important practical issue in extracting intensity-based features is that, FLAIR images of different patients have different ranges of intensities, which may considerably affect the energy of different frequency bands of the wavelet transform. In order to reduce this effect, before computing the wavelet transform, we may divide the gray level values of each hippocampus by its mean or standard deviation. But, this method eliminates the relative intensity information of the right and left hippocampi, which may be an important feature; an abnormal hippocampus is expected to have a lower volume and a higher FLAIR intensity. An alternative method to normalize, while preserving the relative intensity information, is to divide the intensities of each hippocampus by the average intensity of the other hippocampus (i.e. right by left and vice versa). In this case, for each patient the average of intensity ratios will become less than one for the normal hippocampus, and more than one for the abnormal hippocampus (the abnormal one is the brighter one). In this paper, after computing the wavelet transform of each slice and calculating the predefined features (in 2D case), we average the features over all slices. As it is often the case, only one of the hippocampi is abnormal in each patient. To get one set of features for each patient we divide the resulting features of the right hippocampus (i.e. energy, entropy, and volume) by the resulting features of the left hippocampus and use these ratios as the final set of features for each patient.

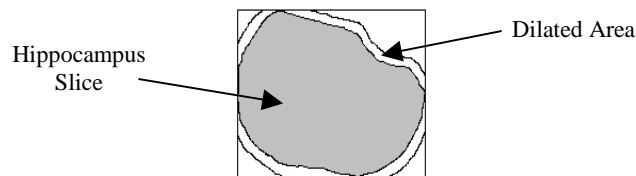


Fig. 5. Filling the empty area by repeated dilations and averaging.

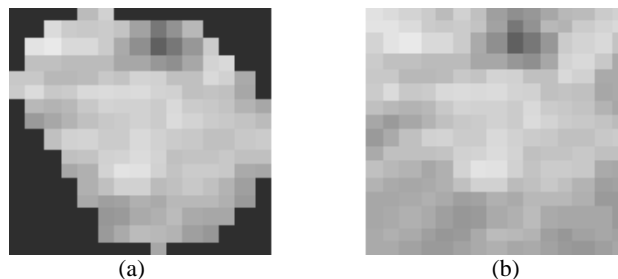


Fig. 6. Segmented hippocampus image, a) before filling the empty area, b) after filling the empty area.

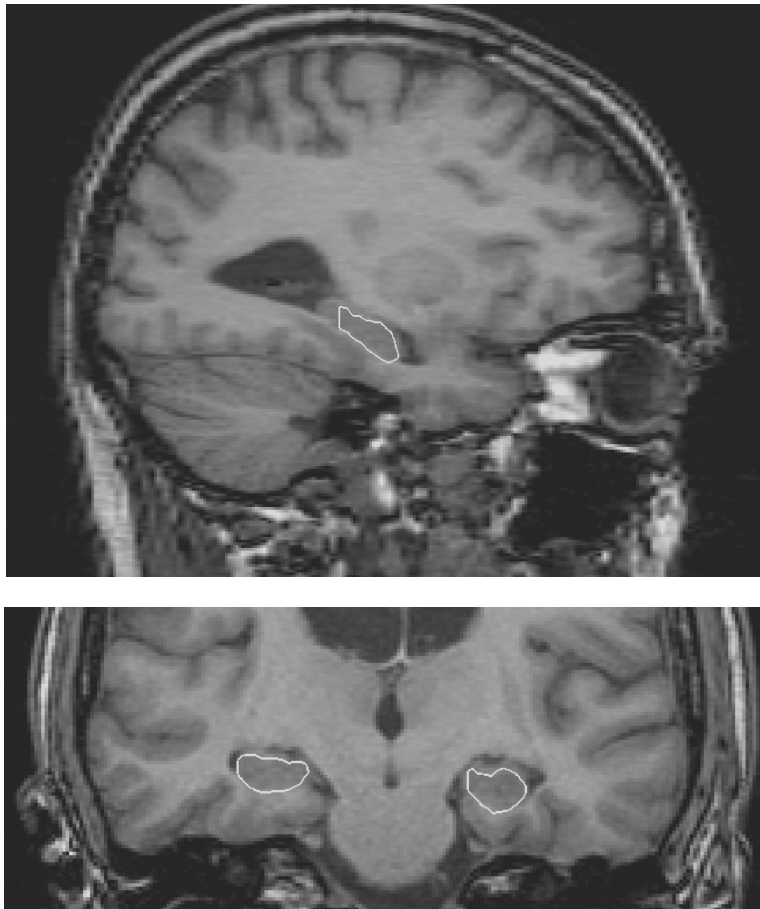


Fig. 7. Sagittal and coronal views of manual segmentation on T1-weighted MR images.

#### 4. EXPERIMENTAL RESULTS

In the experiments, we used the FLAIR images of 20 patients, 10 with right abnormal and 10 with left abnormal hippocampi. Table 1 shows the correct classification percentages using linear classifier with different wavelet bases and feature sets. We used  $D_6$ ,  $D_{20}$  and Biorth2.4 wavelet bases with two levels of decomposition. Energy and entropy ratio features are used separately as well as together for classification. A combination of energy, entropy and volume ratio features is also reported. The features are calculated from the original coronal FLAIR images of the hippocampus as well as the interpolated slices after the hippocampus is rotated to be inscribed in a rectangular prism (noted by “original” and “rotated” respectively). The 2D slices of the hippocampus were used in both original and rotated cases for feature extraction using 2D wavelet decomposition. The 3D image of the rotated volume is also used for feature extraction using 3D wavelet decomposition. As shown in this table, almost all the feature sets lead to 100% correct classification. This means the samples are linearly separable in the feature space. From the linear separability point of view, there is not significant difference between different methods of feature extraction in this table.

Table 2 shows the correct classification percentages using fuzzy c-means clustering algorithm. As shown in this table, the combination of energy and entropy features does not improve the classification rate. According to our experiments, the volume ratio alone provides 90% correct classification using either linear classifier or fuzzy c-means clustering algorithm. But as shown in Table 2, adding volume ratio does not improve the classification rate. From these observations we can conclude that although the samples are linearly separable, the clusters are not far enough from each other to be classified perfectly by fuzzy c-means algorithm. Moreover, as shown in this table the features extracted from

the 2D slices of the rotated volume of hippocampus are generally more discriminative. However, the 3D wavelet decomposition does not provide more information compared with the other methods.

Fig. 8 shows the cluster plots of different energy features of the  $D_6$  wavelet with three different methods of feature extraction mentioned earlier. The “R” and “L” symbols denote the patients with right and left abnormal hippocampi respectively. This figure shows the linear separability of the clusters. The 2D wavelet features in both original and rotated images provide higher separability compared with 3D wavelet features.

Table 1. The correct classification percentages using linear classifier with different wavelet bases and feature sets.

Wavelet Bases	Slices	Features				
		energy	entropy	energy & entropy	energy, entropy & volume	
$D_6$	original	2D	100	100	100	100
	rotated	2D	100	100	100	100
		3D	100	100	100	100
$D_{20}$	original	2D	100	100	100	100
	rotated	2D	100	90	100	100
		3D	100	100	100	100
Boirth2.4	original	2D	100	100	100	100
	rotated	2D	100	95	100	100
		3D	100	100	100	100

Table 2. The correct classification percentages using fuzzy c-means clustering algorithm with different wavelet bases and feature sets.

Wavelet Bases	Slices	Features				
		energy	entropy	energy & entropy	energy, entropy & volume	
$D_6$	original	2D	55	65	55	55
	rotated	2D	80	70	80	80
		3D	70	90	70	70
$D_{20}$	original	2D	80	80	60	60
	rotated	2D	75	55	75	75
		3D	70	85	70	75
Boirth2.4	original	2D	75	65	75	75
	rotated	2D	80	55	80	80
		3D	70	80	70	75

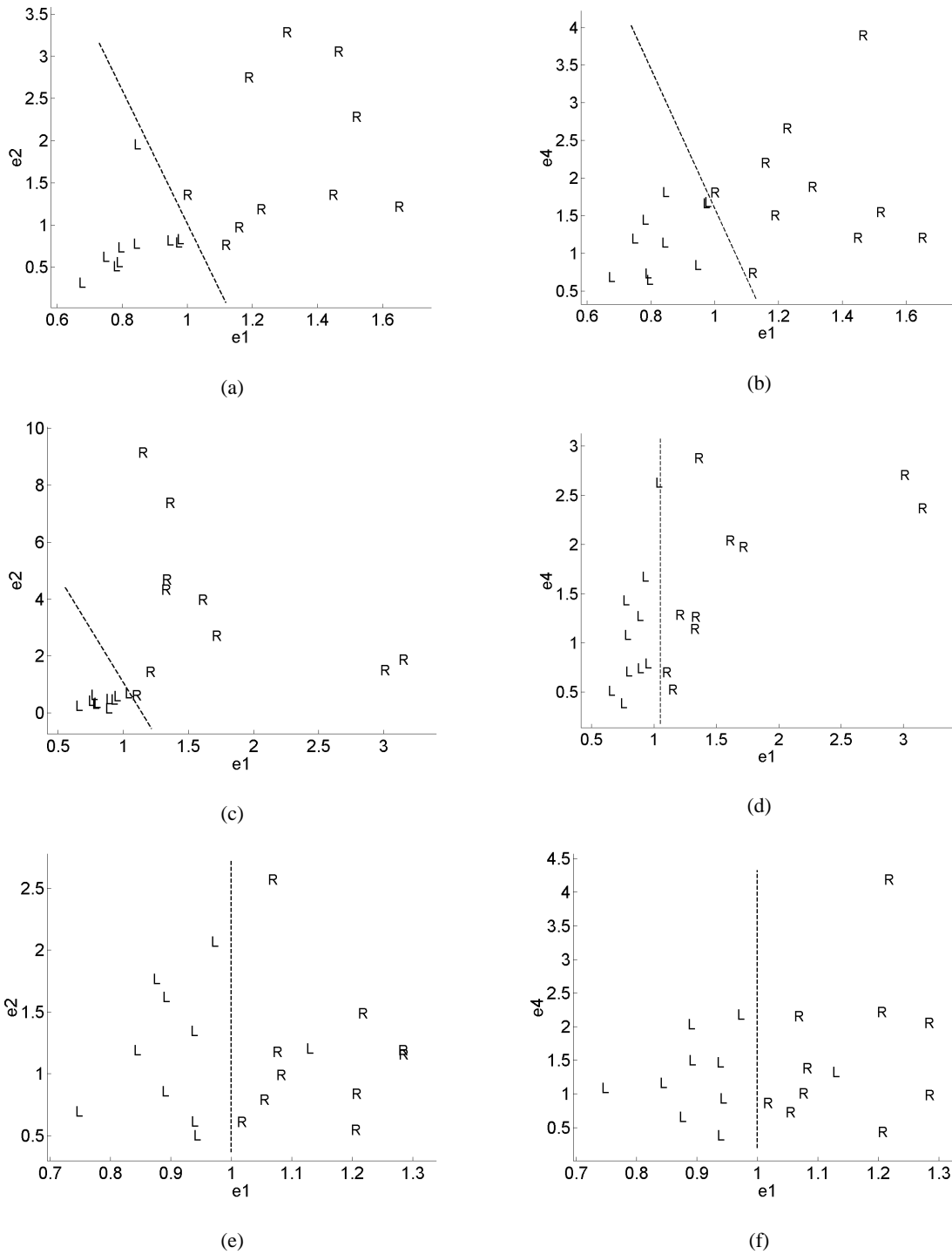


Fig. 8. Cluster plots of energy features from different frequency bands using  $D_6$  wavelet. The “R” and “L” symbols respectively show the patients with right and left abnormal hippocampi (candidates for surgery on the corresponding hippocampus). (a) and (b) using 2D slices of the original images, (c) and (d) using 2D slices of the rotated volume, (e) and (f) using the 3D rotated hippocampus volume.



## 5. SUMMARY AND CONCLUSION

In this work, we used FLAIR images of 20 patients for feature extraction. We have focused on epileptic patients with partial seizures of presumed mesial temporal origin. All patients had EEG records and most of them underwent resection of one of the hippocampi. The location of seizure onset as determined by the EEG methods and the postoperative outcomes were considered as the gold standard. Manual segmentation results from T1-weighted images were mapped to the FLAIR images. Then using the methods explained in Sections 2 and 3 we computed a set of features and then classified them into two groups using linear classifier and fuzzy c-means clustering algorithm. We used  $D_6$ ,  $D_{20}$  and Biorth2.4 bases with two levels of decomposition. The results demonstrate the extracted features are linearly separable and the energy features derived from the 2D wavelet transform provide higher separability compared with 3D wavelet decomposition of the hippocampus.

## REFERENCES

1. C.R. Jack, R.C. Petersen, P.C. O'Brien, and E.G. Tangalos, "MR-based hippocampal volumetry in the diagnosis of Alzheimer's disease", *Neurology*, **42**, no. 1, pp. 183-188, 1992.
2. F. Cendes, F. Andermann, P. Gloor, A. Evans, M. Jones-Gotman, C. Watson, D. Melanson, A. Olivier, T. Peters, I. Lopes-Cendes, and G. Leroux, "MRI volumetric measurement of amygdala and hippocampus in temporal lobe epilepsy", *Neurology*, **43**, no. 4, pp. 719-725, 1993.
3. L. R. Schad, S. Bluml, and I. Zuna, "MR tissue characterization of intracranial tumors by means of texture analysis", *Magnetic Resonance Imaging*, **11**, pp. 889-896, 1993.
4. K. Jafari-Khouzani, M.-R. Siadat, H. Soltanian-Zadeh, and K. Elisevich, "Texture analysis of hippocampus for epilepsy", *Proc. SPIE: Medical Imaging*, 5031, pp. 279-288, Feb. 2003.
5. S. Herlidou, Y. Rolland, J.Y. Bansard, E. Le Rumeur and J.D. De Certaines, "Comparison of automated and visual texture analysis in MRI: characterization of normal and diseased skeletal muscle", *Magnetic Resonance Imaging*, **17**, no. 9, pp. 1393-1397, 1999.
6. S. Herlidou, I. Idy-Peretti, R. Grebe, F. Grados, N. Lecuyer, and P. Fardellone, "Quantitative evaluation of trabecular bone structure by calcaneus MR images texture analysis of healthy volunteers and osteoporotic subjects", *Proc. 23rd Int. Conf. IEEE EMBS*, 3, pp. 2340-2342, 2001.
7. P. Reuze, A. Bruno, and E. Le Rumeur, "Performance evaluation of some textural features for muscle tissue classification", *Proc. Int. Conf. IEEE EMBS*, 1, pp. 645-646, 1994.
8. P.A. Freeborough and N.C. Fox, "MR image texture analysis applied to the diagnosis and tracking of Alzheimer's disease", *IEEE Trans. Medical Imaging*, **17**, no. 3, pp. 475-478, 1998.
9. S. Duchesne, N. Bernasconi, A. Bernasconi, and D.L. Collins, "On the classification of temporal lobe epilepsy using MR image appearance", *Proc. 16th Int. Conf. on Pattern Recognition*, 1, pp. 520-523, 2002.
10. O. Yu, C. Roch, I.J. Namer, J. Chambron, and Y. Mauss, "Detection of late epilepsy by the texture analysis of MR brain images in the lithium-pilocarpine rat model", *Magnetic Resonance Imaging*, **20**, pp. 771-775, 2002.
11. N. Bernasconi, S. B. Antel, and A. Bernasconi, "Texture analysis in mesial temporal lobe epilepsy", *Proc. Int. Mag. Reson. Med.*, **11**, pp. 2021-2021, 2003.
12. N. Bernasconi, S. B. Antel, T. Sankar, and A. Bernasconi, "Quantitative assessment of temporopolar cortex and white matter in temporal lobe epilepsy using volumetric MRI and texture analysis", *Proc. Int. Mag. Reson. Med.*, **11**, pp. 2023-2023, 2003.
13. O. Yu, Y. Mauss, I.J. Namer, and J. Chambron, "Existence of contralateral abnormalities revealed by texture analysis in unilateral intractable hippocampal epilepsy", *Magnetic Resonance Imaging*, **19**, no. 10, pp. 1305-1310, 2001.
14. M. Segovia-Martinez, M. Petrou, and W. Crum, "Texture features that correlate with the mini mental state examination (MMSE) score", *Proc. 23rd Int. Conf. IEEE EMBS*, 3, pp. 2591-2594, 2001.
15. D. Mahmoud-Ghoneim, G. Toussaint, J.-M. Constans, and J.D. de Certaines, "Three dimensional texture analysis in MRI: a preliminary evaluation in gliomas", *Magnetic Resonance Imaging*, **21**, no. 9, pp. 983-987, 2003.
16. S. Herlidou-Même, J. M. Constans, B. Carsin, D. Olivie, P. A. Eliat, L. Nadal-Desbarats, C. Gondry, E. Le Rumeur, I. Idy-Peretti, and J. D. de Certaines, "MRI texture analysis on texture test objects, normal brain and intracranial tumors", *Magnetic Resonance Imaging*, **21**, no. 9, pp. 989-993, 2003.
17. L. Bonilha, E. Kobayashi, G. Castellano, G. Coelho, E. Tinois, F. Cendes, and L.M. Li, "Texture analysis of hippocampal sclerosis", *Epilepsy*, **44**, no. 12, pp. 1546-1550, 2003.
18. S. Mallat, *A wavelet tour of signal processing*, Academic Press, 1999.